A Scalable Design of Multigranularity Optical Cross-Connects for the Next-Generation Optical Internet

Pin-Han Ho, *Member, IEEE*, Hussein T. Mouftah, *Fellow, IEEE*, and Jing Wu, *Member, IEEE*

***Abstract*—This paper proposes a scalable design for next-generation optical cross-connects (OXCs). We present a novel strategy for dimensioning the switching capability as a long term planning. Switching fabrics in OXCs have to be expanded according to traffic growth, which may incur a scalability problem due to the exponentially increasing cost in manufacturing and maintenance. The proposed scheme expands the switching capacity of OXCs with waveband- and fiber-switching components (or, equivalently, expands the network capacity with waveband- and fiber-switching tiers). To minimize the number of extra fibers for waveband- and fiber-switching tiers required to satisfy a given traffic matrix, we formulate the problem of routing and wavelength assignment (RWA) with tunnel allocation (RWAT) into a constraint programming (CP) process. The CP is simplified as two integer linear programming (ILP) processes that are performed sequentially. Experiments are conducted on four examples to compare the throughput and the number of switching points when different switching architectures are adopted under different traffic increase. The benefits of our approach are demonstrated. Finally, we conclude that the proposed optimization scheme can dimension the networks with expandability and scalability to the growing traffic demand.**

***Index Terms*—Generalized multiprotocol label switching (GMPLS), multigranularity, optical cross-connect (OXC), waveband, wavelength-division multiplexing (WDM).**

I. Introduction

With the growth in traffic, more network resources need to be deployed. It is important to expand the total network capacity in a scalable manner. However, simply expanding the switching fabrics that perform lambda switching may cause scalability problem in manufacturing and maintenance, which make costs exponentially growing with the size of switching fabrics. In this paper, we develop an approach that can expand the total switching capacity by equipping the network with tiers of various switching types, i.e., lambda, waveband, and fiber switching. Thus, switching can be done at different traffic granularity. We term the optical cross-connects (OXCs) that can handle multigranularity traffic in the optical domain as multigranularity OXCs (MG-OXCs).

In this paper, we make two key design assumptions. First, the same as the study in [1], we assume the minimum switching unit of a fiber can be either wavelength channels or wavebands, or the entire fiber. Therefore, a fiber can be categorized as lambda, waveband, or fiber switching. Accordingly, input/output ports of MG-OXCs are assigned to one of the three switching types. Links are composed of a number of fibers for different types of switching fabrics.

The second assumption is that each MG-OXC has a fixed number of lambda-switched input/output ports, while the numbers of input/output ports for fiber and waveband switching are subject to design and optimization according to the traffic. The reason is that the lambda-switching devices and modules are far from being scalable in design and manufacturing compared to those for fiber and waveband switching. So, we expand the fiber and/or waveband-switching capacity when the original network cannot accommodate the growing traffic.

Under the above two design assumptions, the network resources to be dimensioned become explicit—the number of fibers in each switching tier, as well as the switching capacity (i.e., the number of input/output ports) in MG-OXCs for each switching type. The dimensioning can either be performed through a programming process, or through a heuristic approach where the whole process includes subtasks that can be solved sequentially. In addition, the traffic matrix will be satisfied through an routing and wavelength assignment (RWA) process after dimensioning the network switching capacity.

The idea of multigranularity traffic in the optical domain with the generalized multiprotocol label switching (GMPLS) control plane has been extensively reported since the early 2000, and the Internet draft devoted to this topic first emerged in mid 2001 [2]. Relevant simulation-based switch architecture design can only be seen in [1] and [3]–[7]. In [4], only qualitative descriptions were provided. In [5], although analysis was presented, it emphasized on point-to-point transmission systems, where traffic grooming was not considered. In [3], the authors considered lightpath bundling in the networks with OXCs that employ two-stage multiplexing switching architecture, or called hierarchical cross-connects (HXCs). The lightpaths from different sources and to the same destination can be bundled as wavebands at intermediate nodes. The design of the HXCs was formulated into an integer linear programming (ILP). However, the design approach in [3] can be further elaborated. First, the

Manuscript received August 1, 2002; revised February 20, 2003.

P.-H. Ho is with Department of Electrical and Computer Engineering, University of Waterloo, Waterloo, ON N2L 3G1, Canada (e-mail: pinhan@bbcr.uwaterloo.ca).

H. T. Mouftah is with School of Information Technology and Engineering, University of Ottawa, Ottawa, ON K1N 6N5, Canada (e-mail: mouftah@site.uottawa.ca).

J. Wu is with Communications Research Center Canada, Ottawa, ON K2H 8S2 , Canada (e-mail: jing.wu@crc.ca).

Digital Object Identifier 10.1109/JSAC.2003.815975

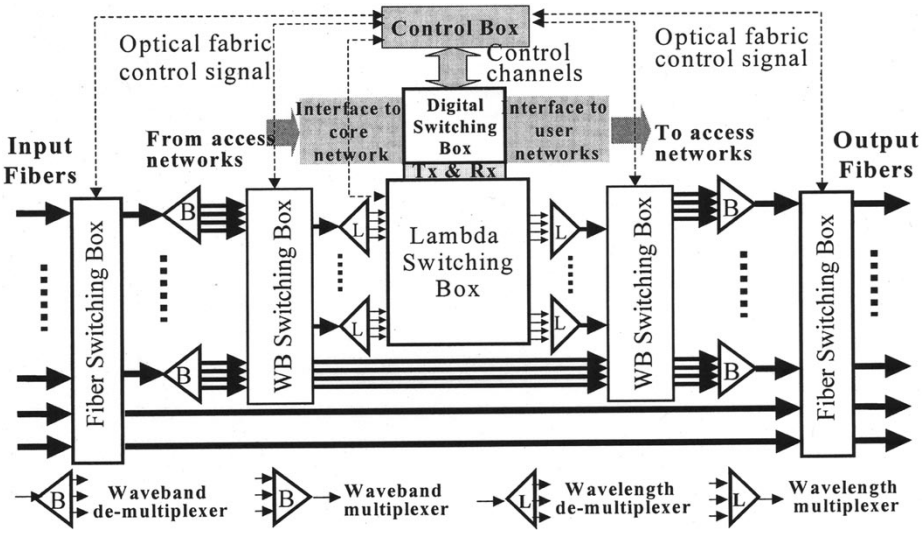

Fig. 1. MG-OXC architecture proposed in [1].

constraint imposed on the lightpath bundling can be relaxed for better capacity efficiency. Second, the number of total switching points in the HXCs can be further reduced by jointly considering fiber-switching tier to explore more possibility of lightpath bundling. In [7], the same switch architecture and design approach as that in [3] were adopted considering the two aspects mentioned above. However, the ILP formulation in [7] suffers from very high computation complexity because all input/output ports need to be numbered even if the fibers are in the same switching tier. In addition, the weighting parameters in the target function of the ILP formulation have never been addressed, which are crucial to optimization results. The heuristic proposed in [7] provides a routing scheme not considering increasing the chance of lightpath bundling. The above facts leave the study in [7] some space to improve.

A different MG-OXC architecture was proposed by us [1], [6], where the lightpath bundling is physically realized by waveband- and fiber-switching components. In [1] and [6], we highlighted the problem of RWAT in MG-OXC networks. We developed three heuristic algorithms for path selection to improve the performance in MG-OXC networks with dynamic traffic, and concluded that the use of MG-OXCs with a proper allocation of different switching types in the network can win the best benefits. However, the previous study was limited to the resource allocation schemes under dynamic traffic, where the switching capacity in each tier was fixed in every node and the number of fibers connected to each switching type along different links was the same. The dimensioning of switching capacity according to growing traffic demand has never been seen in MG-OXC networks.

In this paper, we formulate the RWAT problem into a constraint programming (CP). To reduce the computation complexity induced by the CP formulation, we propose a heuristic approach where the whole optimization process is separated into two ILP processes that can be sequentially performed. Experiments are conducted on the proposed MG-OXC architecture and dimensioning algorithm, followed by a numerical analysis on the total number of switching points in the network.

This paper is organized as follows. In Section II, we introduce the MG-OXC architecture. In Section III, the RWAT problem is formulated into a CP process. In Section IV, a heuristic approach is presented to solve the RWAT problem with much less computation complexity. In Section V, performance is evaluated for the proposed switching architecture. Different strategies for dimensioning the switching capacity are compared. Section VI is the conclusion.

II. MG-OXC Architecture

In this section, we describe the functional architecture and some design issues of MG-OXCs with three tiers in the optical domain (i.e., fiber-, waveband- and lambda-switching tiers).

A. Functional Architecture

The traffic hierarchy in the optical domain has been well defined in the GMPLS control plane [2] and was also described in detail in [1]. This paper adopts the MG-OXC architecture proposed in [1] shown in Fig. 1. The fiber-switching box at the left-hand side dispatches the input fibers to either fiber-, waveband-, or lambda-switching fabrics. The lambda- and waveband-switching boxes and the fiber-switching box on the right-hand side perform space switching at given granularities. The design assumption that each input/output port has a specific switching type simplifies the control and design, which is one of the most distinguishing characteristics in our study from the others.

In Fig. 1, the add–drop multiplexer performs time-division multiplexing on individual lightpaths. In this paper, exchanging time slots without an add–drop operation is not allowed. The subwavelength tier will not be considered in the following discussion since we focus on the optical domain.

B. Tunneling

Our design objective is to dimension the network capacity such that more traffic demand can be accommodated. As the

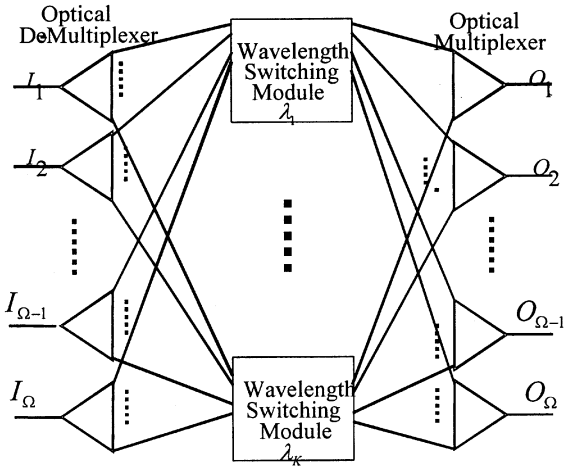

Fig. 2. Lambda-switching OXC with Ω input/output ports.

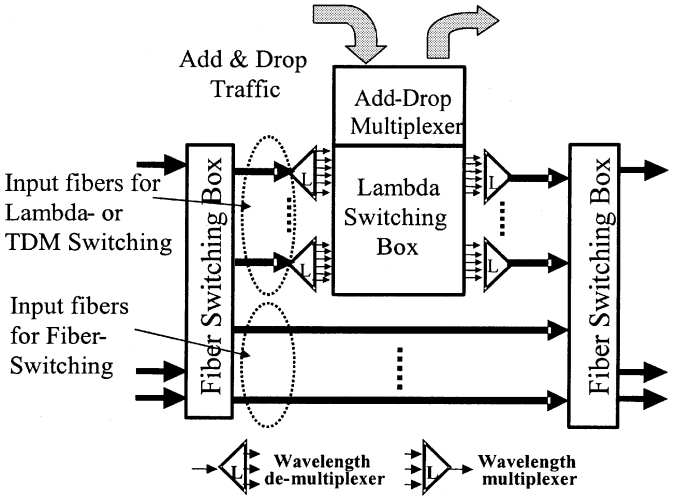

Fig. 3. MG-OXC with only a fiber-switching tier (the waveband-switching tier is absent in this case).

traffic demand increases, the requirement on the switching capacity is increased accordingly. To expand the switching capacity, it is economical to expand the fiber- and/or waveband-switching tiers while keeping the lambda-switching core fixed. Fig. 2 shows an OXC with only lambda-switching capacity. As the traffic demand grows, we can gradually increase the number of input fibers to the OXC that are fiber- or/and waveband-switched, as shown in Figs. 1 and 3.

Since the proposed MG-OXC architecture is no longer nonblocking, virtual connectivity needs to be defined before allocating network resources to lightpath requests. The development of the virtual connectivity in the fiber- and waveband-switching tiers is called a process of *tunneling* [1]. The fiber- and waveband-switching tiers are called *tunnel tiers*. A lightpath with a specific wavelength can take a tunnel if the wavelength channel is free in the tunnel. This can be explained by a simple example in Fig. 4. A fiber tunnel is set up along route A-B-C, where node B allocates one input/output port to the tunnel. In this case, since a fiber from node A has taken the fiber-switching port in node B, no other input fibers to node B can be fiber-switched at this time. In other words, the virtual connectivity in the fiber-switching tier from node D to B does not exist.

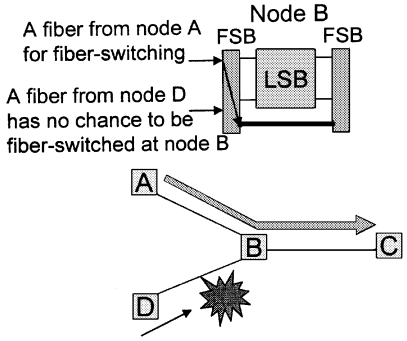

Fig. 4. Tunnel tiers. Lambda-switching box (LSB) and fiber-switching box (FSB).

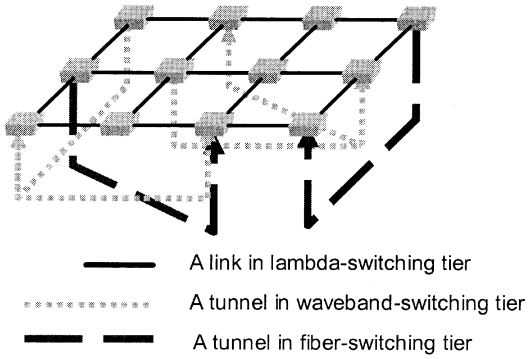

Fig. 5. Illustration for the network topology with tunnels.

The starting and terminating nodes of a tunnel are called the *entry* and *exit* of the tunnel, respectively. As a lightpath goes through a tunnel, it is bundled with other lightpaths having different wavelengths at the *entry* and separated at the *exit*. In this paper, a tunnel can only traverse the shortest path between the corresponding *entry–exit* pair. The network capacity is expanded by having tunnels as extra virtual connections. An example is shown in Fig. 5 for an augmented network.

The *entry–exit* pairs can be jointly determined with the RWA problem through an optimization process, and will be demonstrated in Section III. To reduce computation complexity, a heuristic approach is developed so that the *entry–exit* pairs are determined before the RWA process, and will be introduced in Section IV.

C. Calculation of Switching Points

With the MG-OXC switching architecture, the total size of switching fabrics (or the number of mirrors for the microelectromechanical system (MEMS) devices concerned in this study) is reduced. We assume that two-dimensional (2-D) MEMS technology is used in the switching boxes, where the number of mirrors taken by an $N \times N$ switch is N^2 [8]. The symbols F_b^F, F_b^B, and F_b^L denote the numbers of input/output ports in node b for fiber, waveband, and lambda switching. Assume a fiber contain K wavelengths or B wavebands. Three different switch architectures are studied in this paper, the lambda-switching OXCs (shown in Fig. 2, referred to as configuration Case 1 in this paper), the MG-OXCs (shown in Fig. 1, referred to as configuration Case 2), and the MG-OXCs with only the fiber-switching tier (shown in Fig. 3, referred to as configuration Case 3). The

number of switching points (or, equivalently, the number of mirrors with 2-D flexibility in the MEMS technology, which is symbolized as SSP) for each configuration is

$$\text{SSP}^{\text{Case1}} = K \cdot \Omega^2 \tag{1}$$

$$\text{SSP}^{\text{Case2}} = 2 \cdot \Omega^2 + 2 \cdot B \cdot \left(F_b^B + F_b^L\right)^2 + K \cdot \left(F_b^L\right)^2 \tag{2}$$

$$\text{SSP}^{\text{Case3}} = 2 \cdot B \cdot \Omega^2 + K \cdot \left(F_b^L\right)^2 \tag{3}$$

where $\Omega = F_b^F + F_b^B + F_b^L$. An analysis on the size of switch fabrics with regard to the throughput that can be achieved will be conducted in Section V.

III. Formulation for the RWAT Problem

Based on the MG-OXC architecture introduced above, we formulate the RWAT problem into a CP process, which is characterized by adopting nonbinary variables in the formulation. A network can be represented by Γ, where N, M, and Q are set of nodes, directional links, and source-destination (S-D) pairs that issue traffic, respectively. The optimization objective is to satisfy a traffic matrix Λ, which specifies the traffic demand (or the number of lightpaths to be setup) for each S-D pair. Note that a lightpath is directional and, thus, Λ may not be symmetrical. According to the second design assumption mentioned in Section I, the number of fibers witch switching granularity of lambda (i.e., F_b^L) is fixed in any node b; however, the numbers of fibers for waveband and fiber switching (i.e., F_b^B and F_b^F, respectively) are adaptive to the given traffic matrix, and will be determined in the optimization process. The number of fibers in the tunnel tiers along each directional link also needs to be determined. Assume that all tunnels have lengths in hops greater than or equal to the average distance in a network. This is important to reduce the resource fragmentation in the tunnel tiers [1]. All node-pairs with a distance larger than or equal to the average distance of the network have been collected into node-pair set V. Some other variables are defined as follows:

- $\lambda_{s,d,k}$: number of lightpaths connecting node-pair (s,d) on wavelength k;
- $\Lambda_{s,d}$: number of lightpaths demanded from node s to node d;
- $L_{s,d,k}^{a,b}$: number of lightpaths in the lambda-switching tier connecting node pair (s,d) and traversing link $a-b$ on wavelength k;
- $FI_{b,k}$, $FO_{b,k}$: are the numbers of lightpaths flowing into/out of node b that are fiber-switched, respectively;
- $BI_{b,k}$, $BO_{b,k}$: are the numbers of lightpaths flowing into/out of node b that are waveband-switched, respectively;
- $\delta B_{p,k}^{r,z}$, $\delta F_p^{r,z}$: are the numbers of waveband tunnels on wavelength k and fiber tunnels with the *entry* and *exit* at node r and z, and taking the pth shortest path between r and z;
- $f_{a,b}^F$, $f_{a,b}^B$, $f_{a,b}^L$: are the numbers of fibers for fiber, waveband, and lambda switching along link $a-b$;
- $\xi_{r,z,p}^{a,b}$: binary indicator which is 1 if the p-*th* shortest path between node-pair (r,z) passes link $a-b$ and zero, otherwise;
- $SP(r,z)$: returns the set of shortest paths for node pair (r,z).

The optimization is formulated as a CP process shown below

$$\text{Minimize} \sum_b F_b^F + \alpha \cdot \sum_b F_b^B \tag{4}$$

subject to the following constraints:

$$F_b^F = \sum_a f_{a,b}^F = \sum_c f_{b,c}^F \quad \text{for any node } b \in N \tag{5}$$

$$F_b^B = \sum_a f_{a,b}^B = \sum_c f_{b,c}^B \quad \text{for any node } b \in N \tag{6}$$

$$\sum_a L_{s,d,k}^{a,b} + FI_{b,k} + BI_{b,k} - \sum_c L_{s,d,k}^{b,c} - FO_{b,k} - BO_{b,k} = \begin{cases} -\lambda_{s,d,k}, & \text{if } s = b \\ \lambda_{s,d,k}, & \text{if } d = b \\ 0, & \text{otherwise,} \end{cases}$$
$$\text{for any node } b \in N \text{ and } (s,d) \in Q \tag{7}$$

$$0 \le FI_{b,k} \le \sum_{(r,b)\in V} \sum_{p \in SP(r,b)} \delta F_p^{r,b}, \quad \text{for } b \in N \text{ and wavelength } k \tag{8}$$

$$0 \le BI_{b,k} \le \sum_{(r,b)\in V} \sum_{p \in SP(r,b)} \delta B_{p,k}^{r,b}, \quad \text{for } b \in N \text{ and wavelength } k \tag{9}$$

$$0 \le FO_{b,k} \le \sum_{(b,z)\in V} \sum_{p \in SP(b,z)} \delta F_p^{b,z}, \quad \text{for } b \in N \text{ and wavelength } k \tag{10}$$

$$0 \le BO_{b,k} \le \sum_{(b,z)\in V} \sum_{p \in SP(b,z)} \delta B_{p,k}^{b,z}, \quad \text{for } b \in N \text{ and wavelength } k \tag{11}$$

$$f_{a,b}^F = \sum_{(r,z)\in V} \sum_{p \in SP(r,z)} \delta F_p^{r,z} \cdot \xi_{r,z,p}^{a,b}, \quad \text{for link } a-b \in M \tag{12}$$

$$f_{a,b}^B \ge \frac{B}{K} \cdot \sum_{(r,z)\in V} \sum_{p \in SP(r,z)} \sum_{k=((t-1)\cdot K/B)}^{t\cdot K/B-1} \delta B_{p,k}^{r,z} \cdot \xi_{r,z,p}^{a,b}, \quad \text{for link } a-b \in M \text{ and } t = 1 \sim B \tag{13}$$

$$f_{a,b}^L \ge L_{s,d,k}^{a,b}, \quad \text{for link } a-b \in M \tag{14}$$

$$0 \le f_{a,b}^F + f_{a,b}^B \le H, \quad \text{for link } a-b \tag{15}$$

$$\sum_k \lambda_{s,d,k} = \Lambda_{s,d}, \quad \text{for } (s,d) \in Q. \tag{16}$$

The target function (4) aims to minimize the switching capacity that needs to be expanded in the fiber- and waveband-switching tiers. A factor α reflects the fact that the cost of expanding input/output ports for fiber- and waveband-switching is different. Equation (5) or (6) stipulates that the switching capacity of a specific type in a node should be equal to the sum of all input (or output) fibers to (or from) the node for that switching type. Equation (7) shows the equilibrium of traffic flows entering and leaving a node on a wavelength. These are called the flow conservation constraints. An example is shown in Fig. 6, where the fiber-, waveband-, and lambda-switched fibers entering node b should be the same as the switching capacity of each type in node b. Equations (8) and (9) [or (10) and

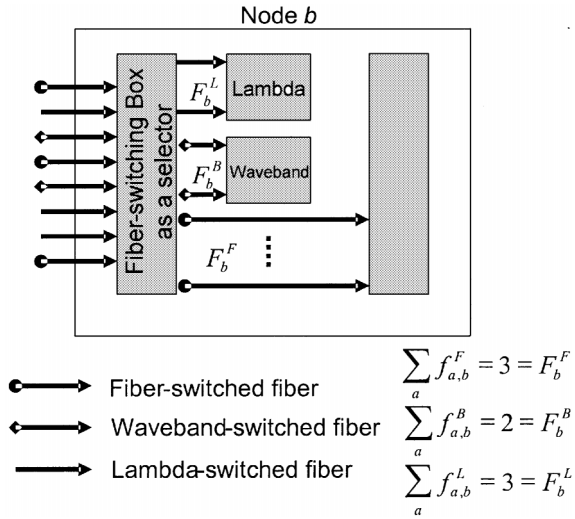

Fig. 6. Example showing the capacity in each switching tier of node b, where $b \in N$. The number of fiber-, waveband-, and lambda-switched fibers entering node b is 3, 2, and 3, respectively.

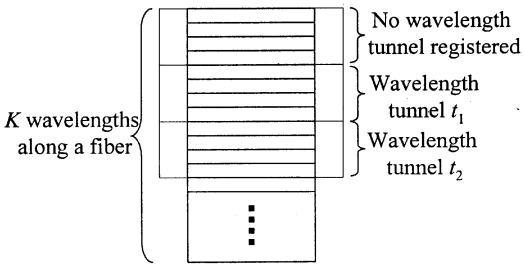

Fig. 7. Example for (13).

(11)] impose an upper bound on the number of lightpaths on wavelength k that possibly enter (or leave) node b, which is the number of tunnels to be established. Equation (12) describes the relationship between the number of fiber-switched fibers along a link and the fiber tunnels that can be supported along that link. Equation (13) imposes an upper bound on the number of waveband tunnels along a link that can be supported by the waveband-switched fibers on that link. It is an upper bound as opposed to an exact value in (12) because a waveband-switched fiber can support up to B waveband tunnels, while each fiber-switched fiber is lighted up for a single fiber tunnel. A factor (B/K) is required in (13) because an entire band of wavelength is summed for each link, which yields (K/B) times of desired value. Fig. 7 shows an example. Assume only two out of B wavebands are taken as waveband tunnels along the fiber. Note that each waveband has (K/B) wavelength channels. In case only a single fiber is for waveband-switching, (13) returns $(2 \cdot K/B)$ when we sum up each tunnel t for each wavelength plane in the fiber. Therefore, we must factor the summation result by (B/K) to derive the number of waveband tunnels along this fiber. Equation (14) imposes an upper bound on the number of lightpaths that are lambda-switched along a link. Equation (15) is necessary if any upper bound H is imposed on the number of total fibers along link $a-b$. Equation (16) describes that the traffic demand for an S-D pair should be the sum of traffic flows between the S-D pair on all wavelength planes.

IV. Heuristic Approach

To reduce the computation complexity induced by the CP formulation, a heuristic approach is developed to design MG-OXCs. The CP is approximated by three subtasks that can be handled sequentially. The first subtask is to determine the *entries* and *exits* of all tunnels. The second is to perform an RWA process to route lightpath requested in the traffic matrix and assign wavelengths. The third is to select physical routes for all tunnels selected in the first subtask. Then the number of fibers for each switching type is determined. If the entire traffic matrix cannot be satisfied in the RWA process, more tunnels will be arranged by repeating the first subtask.

A. Selection of Entry–Exit Pairs

The extra traffic demand is calculated as the offset of traffic matrix $\Delta\Lambda = \Lambda' - \Lambda$, where Λ' is the new traffic matrix. Some elements in $\Delta\Lambda$ may be negative. $\Delta\Lambda_{n,m}$ is the offset of traffic demand for node pair (n, m).

Recall that all the node pairs with at least the average hop in a network are stored in set V. To select *entry–exit* pairs for V, we define *potential* of a node- pair

$$P_{r,z} = \Delta\Lambda_{r,z} + \sum_{n \in \tilde{r}_h} \sum_{m \in \tilde{z}_g} (\chi_{h,g} \cdot \Delta\Lambda_{n,m}) \text{ for } (r,z) \in V \tag{17}$$

where $\tilde{r}_h$ and $\tilde{z}_g$ are defined as the node sets containing all the nodes with h and g hops away from node r and z, respectively; $\chi_{h,g}$ is a parameter which evaluates the likelihood for the traffic demand of a node pair to take a tunnel, where the source and destination of the node pair are h and g hops away from the *entry* and *exit* of the tunnel, respectively. In this paper

$$\chi_{h,g} = (h+g+1)^{-1/2} \tag{18}$$

$\underset{all(r,z)}{i\text{Max}}\,(P_{r,z})$ denotes node pair (R, Z) with maximum potential, i.e., $P_{R,Z} = \max\limits_{all(r,z)} (P_{r,z})$. The heuristic algorithm is described as follows.

Input: $\Delta\Lambda$;
Output: Set S containing the *entry–exit* pairs for all tunnels. Note that multiple tunnels may have the same *entry–exit*.
Step 1: Find $P_{r,z}$ according to $\Delta\Lambda$ for all $(r,z) \in V$;
Step 2: If $\max\limits_{all(r,z)} (P_{r,z}) < 0$, algorithm stops;
Step 3: $(R,Z) \leftarrow \underset{all(r,z)}{i\text{Max}}\,(P_{r,z})$; If $P_{R,Z} > K$, add (R,Z) into set S as a fiber tunnel, where K is the number of wavelength channels supported in a fiber; else if $K > P_{R,Z} > 0$, add (R,Z) into set S as a waveband tunnel;
Step 4: When a fiber tunnel (or a waveband tunnel) is added into the set S, randomly remove K or (K/B) lightpath requests from the elements (n,m) in the offset traffic matrix $\Delta\Lambda_{n,m}$, where $n \in \tilde{r}$ and $m \in \tilde{z}$.
Step 5: Go to Step 1.

Note that the selection process does not assign wavelengths. In other words, the waveband tunnels have not been assigned a specific wavelength range. The task of wavelength assignment for the waveband tunnels will be conducted in the RWA process introduced in the next section. The parameter $\chi_{h,g}$ plays a key

role to determine the location of the *entry* and *exit* of tunnels, which consequently determines network throughput.

B. RWA

Network capacity is increased by additional tunnels in the fiber and waveband tiers. Given the endpoints of all *entry–exit* pairs, the RWA process can be performed by ILP or heuristic algorithms. This paper introduces an ILP formulation as follows:

$$\text{Minimize} \sum_{all(s,d)} \Lambda_{s,d} - \sum_{k} \lambda_{s,d,k} \tag{19}$$

subject to the following constraints:

$$\sum_{a} T^{a,b}_{s,d,k} - \sum_{c} T^{b,c}_{s,d,k} = \begin{cases} -\lambda_{s,d,k}, & \text{if } b = d \\ \lambda_{s,d,k}, & \text{if } b = s \\ 0, & \text{otherwise,} \end{cases} \quad \text{for } b \in N \text{ and all } k \tag{20}$$

$$T^{a,b}_{s,d,k} = L^{L}_{a,b}, \quad \text{if } a, b \in N \text{ and are adjacent} \tag{21}$$

$$T^{a,b}_{s,d,k} \le \sum_{t} (\sigma B^{t}_{a,b,k} + \sigma F^{t}_{a,b}), \quad \text{if } a, b \in N \text{ and are not adjacent} \tag{22}$$

$$F^{B}_{b} \ge \frac{B}{K} \cdot \sum_{t} \sum_{a} \sum_{k=(i-1)K/B}^{(i \cdot K/B)-1} \left(\sigma B^{t}_{a,b} \cdot \tau^{t}_{k}\right), \quad \text{for } b \in N, \text{ and } i \text{ is an integer ranging from 1 to } B \tag{23}$$

where $T^{a,b}_{s,d,k}$ is the number of the lightpaths observed by the lambda-switching devices in node b. Note that $T^{a,b}_{s,d,k}$ is the sum of all traffic flows directly entering node b from node a, which traverses either a single wavelength channel or a tunnel; $\sigma B^{t}_{a,b}$ is a binary indicator which is 1 if the tth tunnel defined in set S is a waveband tunnel with an *entry–exit* pair (a, b) and zero, otherwise; τ^{t}_{k} is a binary variable which takes value 1 if the sth tunnel is waveband-switched containing wavelength k and zero, otherwise; $\sigma F^{t}_{a,b}$ is a binary indicator which is 1 if the tth tunnel defined in set S is a fiber tunnel with an *entry–exit* pair (a, b), and zero, otherwise.

The objective function (19) is to minimize the number of lightpath requests that cannot be satisfied. Equation (20) describes the equilibrium of the number of the lightpaths entering and leaving node b that are lambda-switched on any wavelength. The lightpaths can either enter/leave the node's lambda-switching tier through a wavelength channel or through an *Entry*/*Exit* of a tunnel. $T^{a,b}_{s,d,k}$ is constrained by (21) and (22) for the cases where nodes a and b are adjacent and nonadjacent, respectively. Equation (23) imposes another constraint to facilitate wavelength assignment for the waveband tunnels defined in set S.

If some lighpath demands cannot be satisfied through the above ILP process, the network capacity must be further increased. In this case, the traffic demand that cannot be satisfied is taken to form a new offset traffic matrix $\Delta\Lambda$, and more tunnels are added by using the procedure described in the previous section. Then, the ILP is performed again with additional *Entry-Exit* pairs. The iterative process does not stop until all lightpath requests are satisfied, or until a tolerable amount of residual traffic demand is left unsatisfied.

C. Tunnel Allocation

The *entry–exit* pairs decide the switching capacity required in the fiber- and waveband-switching tiers. We must also determine the physical routes for those tunnels so that the number of fibers for a switching type along each link can be determined. This task is equivalent to solve $f^{B}_{a,b}$ and $f^{F}_{a,b}$ for link $a-b \in M$ in the programming process in Section III. We assume that the cost of taking a fiber for fiber and waveband switching along link $a-b$ is $C^{F}_{a,b}$ and $C^{B}_{a,b}$. The tunnel allocation can be formulated into an ILP

$$\text{Minimize} \sum_{all a-b \in M} \left(C^{B}_{a,b} \cdot f^{B}_{a,b} + C^{F}_{a,b} \cdot f^{F}_{a,b}\right) \tag{24}$$

subject to the following constraints:

$$f^{F}_{a,b} = \sum_{s} \xi F^{t}_{p} \cdot \pi^{p,t}_{a,b}, \text{ for all link } a-b \in M \tag{25}$$

$$f^{B}_{a,b} \ge \frac{B}{K} \cdot \sum_{t} \sum_{k=(i-1)\cdot K/B}^{(i \cdot K/B)-1} \left(\xi B^{t}_{p} \cdot \pi^{p,t}_{a,b} \cdot \tau^{t}_{k}\right), \quad \text{for } i = 1 \text{ to } B \text{ and all link } a-b \in M \tag{26}$$

$$F^{F}_{b} = \sum_{a} f^{F}_{a,b} = \sum_{a} f^{F}_{b,a}, \text{ for } b \in N \tag{27}$$

$$F^{B}_{b} = \sum_{a} f^{B}_{a,b} = \sum_{a} f^{B}_{b,a}, \text{ for } b \in N \tag{28}$$

$$f^{F}_{a,b} + f^{B}_{a,b} \le H, \text{ for all link } a-b \in M \tag{29}$$

where ξF^{t}_{p} (or ξB^{t}_{p}) is a binary variable which is 1 if the tth tunnel in the set S is a fiber (or a waveband) tunnel and takes the pth shortest path between its *entry–exit* pair and zero, otherwise; $\pi^{p,t}_{a,b}$ is a binary indicator which is 1 if the pth shortest path of the tth tunnel in the set S passes link $a-b$ and zero, otherwise; τ^{t}_{k} is a binary indicator which is 1 if the tth tunnel in the set S is a waveband tunnel containing wavelength k. The target function (24) is to minimize the total cost of laying fibers for fiber and waveband switching in each link. Equation (25) relates the number of fibers for fiber switching on link $a-b$ with the selection of physical routes for all the fiber tunnels. Equation (26) means that the number of fibers for waveband-switching is the maximum number of waveband tunnels on the same link with a specific wavelength range. For example, if a link contains ten waveband tunnels with a specific wavelength range, we have to prepare at least ten fibers on this link for waveband switching. Equations (27)–(29) are the same as (5), (6), and (15).

The flowchart in Fig. 8 summarizes the proposed heuristic approach.

V. Performance Evaluation

A. Verification of the Heuristic Approach

To verify the heuristic approach, we compared the results from the CP in Section III, which is solved by the CPLEX mixed integer optimizer. We also use ILOG CPLEX simplex optimizers with SUN WorkStation Ultra 10 (with 1-GB memory)

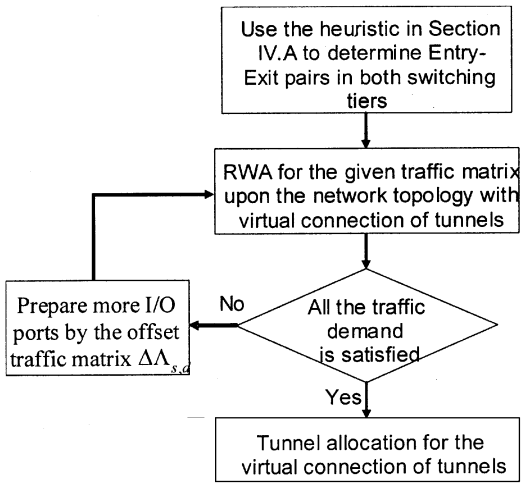

Fig. 8. Flowchart for the proposed heuristic approach to solve RWAT.

to solve the ILP formulations in Sections IV-B and IV-C (for more information about CPLEX see the ILOG CPLEX Advanced Reference Manual [9]). Due to the very high computation complexity, a 10-node network shown in Fig. 9(a) was tested with $K = 8$ and $B = 4$. The original network has two fibers for lambda switching in each link. Despite this, the computation takes around four days.

The experiment procedure is described as follows. The network was first loaded with random traffic of lightpaths one by one until ten consecutive blocking occurs, from which the traffic matrix Λ was formed. Then, we generated a new traffic matrix $\Lambda'_{s,d} = [\Lambda_{s,d} \cdot (1 + \theta \cdot d\%)]$ for all $(s, d) \in Q$, where θ is a random fluctuation which is set $0.5 < \theta < 1.5$, d is the average percentage value of traffic increase, and the operator $[\cdot]$ returns the maximum integer smaller than the operand. We also prepared all the shortest paths for each node pair in the network. The results were averaged over ten independent experiments using different traffic matrices generated through the same procedure and parameter d. The number of the original input/output ports is 60. The constant α in (4) is set to B, which is 4 in this experiment. The constants $C^F_{a,b}$ and $C^B_{a,b}$ are set to 1 for all link $a - b$, which means that no difference exists in the cost to lay down a fiber for fiber-switching or waveband-switching. Table I lists the number of input/output ports that need to be added into the network to satisfy the growing traffic demand. The link utilization in each switching tier has a difference within 5%.

From Table I, we observed that the solution by the heuristic approach is within 10% of that of the CP formulation, and can be accepted as a good approximation to the optimization solution. We also found that the ratio between the numbers of extra input/output ports for the waveband- and fiber-switching tiers is much determined by the constant c and the value of B for the CP formulation case and for the heuristic approach case, respectively. Since we set $\alpha = B$, the two schemes thus yield a similar ratio of switching capacity in the waveband- and fiber-switching tiers (roughly two).

B. Performance Evaluation of Examples

The heuristic approach is further evaluated on four examples (shown in Fig. 9). The 10-node and 16-node networks in Fig. 9(a) and (b) are densely meshed with a nodal degree no less than 3. The 19- and 12-node networks in Fig. 9(c) and (d) are sparsely meshed with a nodal degree 2.63 and 2.33, respectively. The 12-node network in Fig. 9(d) can be an expansion of a star or ring architecture, which is largely adopted in nowadays commercial applications. The main purpose of the experiments is to compare the networks with lambda-switching OXCs and with the MG-OXCs in term of the number of total extra input/output ports required to satisfy the given traffic demand. In addition, an observation is made on the influence of network topology upon the arrangement of different switching types. We will only focus on the analysis the switching architecture with the 2-D MEMS technology, where the total number of mirrors in the networks is of interest.

In the simulation, the networks use 16 wavelengths in a fiber. Originally, five lambda-switched fibers are allocated to each link. A waveband is defined as four wavelength channels consecutive in wavelength. Therefore, wavelengths 1–4, 5–8, 9–12, and 13–16 are in the first, second, third, and fourth waveband, respectively. No wavelength conversion is applied. For the comparison purpose, we also use the ILP formulation introduced in [10] to deal with the RWA problem in pure lambda-switched networks. The construct of the network environment is through the same approach adopted in the experiment in Section V-A.

Tables II–V show the number of extra input/output ports required in the four networks to accommodate the increasing traffic demand (i.e., 1.2, 1.4, 1.6, and 1.8 times of the original traffic demand in average). The traffic matrix is increased by 20%, 40%, 60%, and 80% (i.e., $d = 20$, 40, 60, and 80, respectively) in each case.

From the experiment results it is clear that as the traffic demand increases, the number of input/output ports in the networks must be increased roughly in proportion. The amount of increase of the input/output ports depends on the network topology and also the switch architecture. The networks expanded with pure lambda-switching capacity (i.e., Case 1) need the least amount of total extra input/output ports, however, the networks expanded with pure fiber-switching capacity need the largest number of input/output ports. We attribute this result to the less wavelength-hop utilization in the fiber- and waveband-switching tiers in Case 2 and Case 3. The less wavelength-hop utilization is incurred by the adoption of larger switching granularity. The same result has also been reported in [1].

The adoption of the waveband-switching tier (i.e., Case 2) improves the case with only the fiber-switching tier (i.e., Case 3) by saving more input/output ports. Case 2 takes much less number of input/output ports especially when the networks were sparsely meshed (e.g., the 12-node network), in which more than 60% of reduction in the number of extra ports is achieved. However, this effect becomes less significant as the network becomes densely meshed. As shown in the experiments for the 10- and 16-node networks (Tables II and III), the difference in the number of extra input/output ports is around 20% between Case 2 and Case 3. The lightpaths in the sparsely meshed networks consume more wavelength hops in order to fit into tunnels due to the poor connectivity in the networks, which worsens the resource utilization.

The less input/output ports required in the networks of Case 1 is at the expense of taking more switching points in the OXCs. The percentage of increase in the total number of extra mirrors required in the networks, $\delta\mathrm{SPP}$ can be determined by

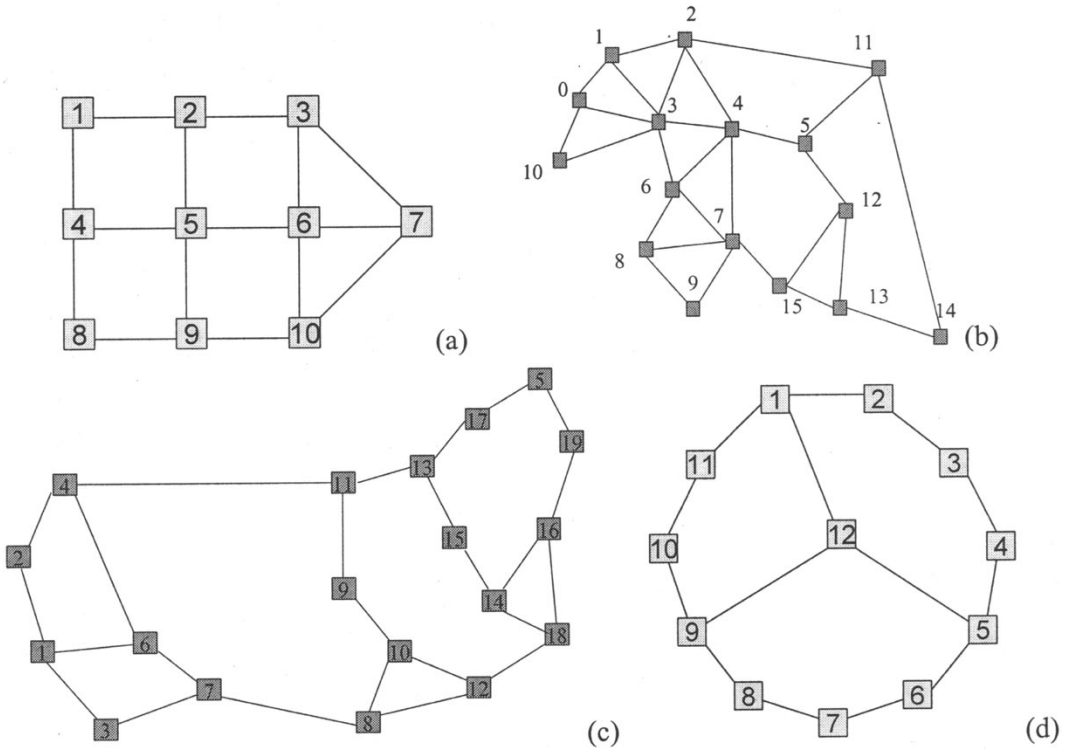

Fig. 9. The four examples with 10, 16, 19, and 12 nodes adopted in the study. The minimum lengths of tunnels for the three networks are 2, 3, 3, and 3 hops, respectively.

TABLE I
COMPARISON BETWEEN THE RESULTS BY THE CP FORMULATION AND BY THE HEURISTIC APPROACH

	CP Formulation			Heuristic		
	Fiber	Waveband	Total	Fiber	Waveband	Total
$d = 50$	20	9	29	21	10	31
$d = 100$	41	19	60	43	20	63

TABLE II
NUMBER OF EXTRA INPUT/OUTPUT PORTS IN THE 10-NODE NETWORK WHERE THE TOTAL NUMBER OF ORIGINAL INPUT/OUTPUT PORTS IS 150 (Average Nodal Degree = 3.00)

	Case 1 Lambda	Case 2			Case 3 Fiber
		Waveband	Fiber	Total	
$d = 20$	30 (20.0%)	10 (6.7%)	23 (15.3%)	33 (22.0%)	42 (28.0%)
$d = 40$	57 (39.0%)	23 (15.3%)	41 (27.3%)	64 (42.6%)	83 (55.3%)
$d = 60$	88 (58.7%)	35 (23.3%)	61 (40.7%)	96 (64.0%)	123 (82.0%)
$d = 80$	117 (78.7%)	41 (27.3%)	88 (58.7%)	129 (86.0%)	161 (107.3%)

TABLE III
NUMBER OF EXTRA INPUT/OUTPUT PORTS IN THE 16-NODE NETWORK WHERE THE TOTAL NUMBER OF ORIGINAL INPUT/OUTPUT PORTS IS 270 (Average Nodal Degree = 3.38)

	Case 1 Lambda	Case 2			Case 3 Fiber
		Waveband	Fiber	Total	
$d = 20$	53 (19.6%)	21 (7.8%)	40 (14.8%)	61 (22.6%)	81 (30.0%)
$d = 40$	101 (37.4%)	36 (13.3%)	79 (29.3%)	115 (42.6%)	158 (58.5%)
$d = 60$	150 (55.6%)	56 (20.7%)	117 (43.3%)	173 (64.1%)	237 (87.8%)
$d = 80$	208 (77.0%)	81 (30.0%)	151 (55.9%)	232 (85.9%)	315 (116.7%)

TABLE IV
NUMBER OF EXTRA INPUT/OUTPUT PORTS IN THE 19-NODE NETWORK WHERE THE TOTAL NUMBER OF ORIGINAL INPUT/OUTPUT PORTS IS 250 (Average Nodal Degree = 2.63)

	Case 1 Lambda	Case 2			Case 3 Fiber
		Waveband	Fiber	Total	
$d = 20$	47 (18.8%)	19 (7.6%)	37 (14.8%)	56 (22.4%)	82 (32.8%)
$d = 40$	93 (37.2%)	33 (13.2%)	71 (28.4%)	104 (41.6%)	160 (64.0%)
$d = 60$	140 (56.0%)	51 (20.4%)	105 (42.0%)	156 (62.4%)	237 (94.8%)
$d = 80$	192 (76.8%)	72 (28.8%)	140 (56.0%)	212 (84.8%)	321 (128.4%)

TABLE V
NUMBER OF EXTRA INPUT/OUTPUT PORTS IN THE 12-NODE NETWORK WHERE THE TOTAL NUMBER OF ORIGINAL INPUT/OUTPUT PORTS IS 140 Average Nodal Degree = 2.33)

	Case 1 Lambda	Case 2			Case 3 Fiber
		Waveband	Fiber	Total	
$d = 20$	29 (20.7%)	12 (8.6%)	22 (15.7%)	34 (24.3%)	51 (36.4%)
$d = 40$	57 (40.7%)	24 (17.1%)	44 (31.4%)	68 (48.6%)	112 (80.0%)
$d = 60$	84 (60.0%)	35 (25.0%)	65 (46.4%)	100 (71.4%)	178 (127.1%)
$d = 80$	114 (81.4%)	46 (32.9%)	87 (62.1%)	133 (95.0%)	211 (150.7%)

the expressions in (1)–(3). We use the following three equations to obtain δSPP in each case as shown in (30)–(32), at the bottom of the next page, where Ω_b^0 and Ω_b is the number of total input/output ports to node b, before and after the switching capacity is expanded, respectively. By observing (30)–(32), it is clear that Case 2 and Case 3 need much less switching points than Case 1 because of the factor K in the denominator. In addition, Case 2 may take a significantly more switching points than Case 3 if the factor B is large. We plot δSSP versus the increase in traffic demand in Fig. 10(a) and (b) using (30)–(32) for all networks.

The analysis results in Fig. 10 show that Case 1 requires an increasing amount of extra switching points much faster than that of the other two cases in all examined network topologies

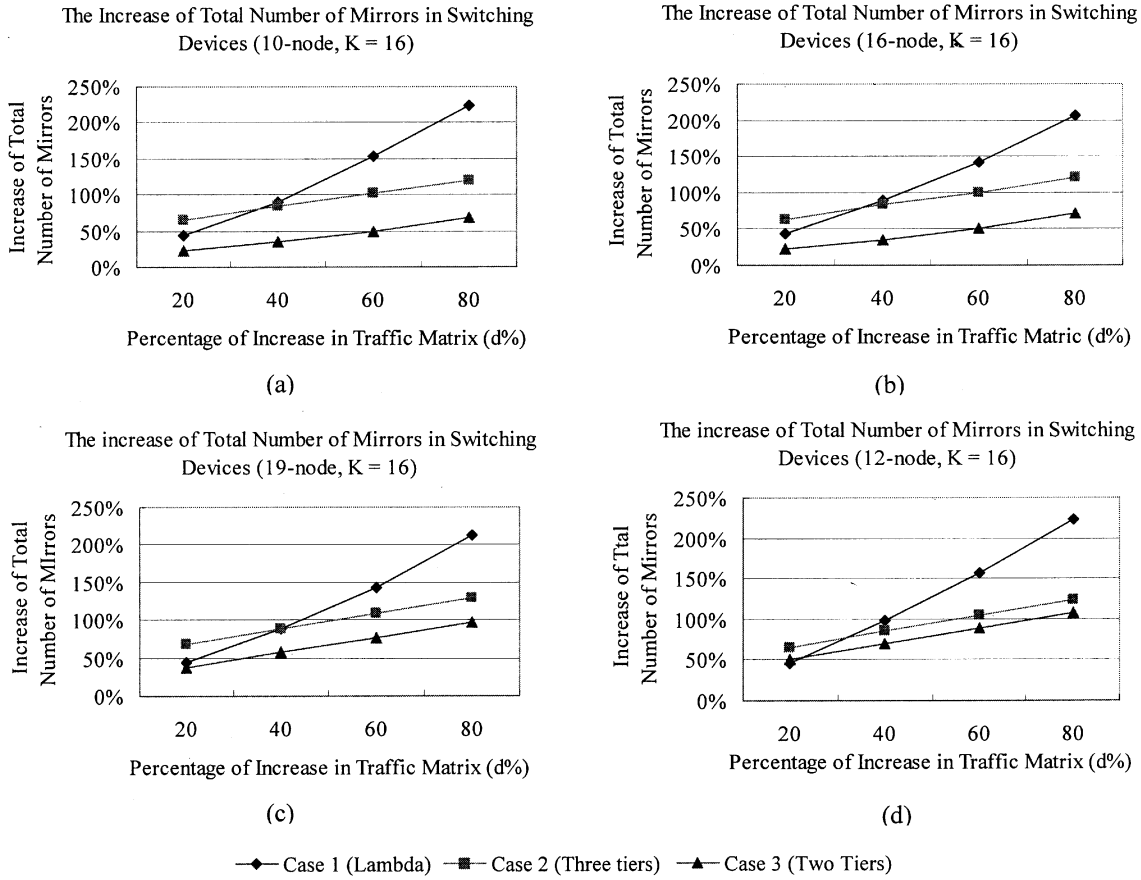

Fig. 10. Increase of total number of mirrors (in percentage) corresponding to the increase of traffic demand for the three cases and the four networks examined in this study; (a), (b), (c), and (d) are for 10-, 16-, 19-, and 12-node networks with a nodal degree 3.0, 3.38, 2.63, and 2.33, respectively.

as the traffic is growing, and most likely suffers from scalability problem. Note that the cost of manufacturing and maintenance for the switching fabrics can be exponentially increased with the number of mirrors. We also observe that the use of the waveband-switching tier (i.e., Case 2) takes only a very limited amount of extra switching points as traffic is growing compared with Case 3 in which a much larger number of extra input/output ports are consumed.

In summary, the proposed MG-OXC architecture can effectively reduce the number of switching points as the traffic demand grows, while at the expense of a moderate increase (i.e., $5\% \sim 15\%$) in the number of input/output ports. In general, the adoption of the waveband-switching tier can benefit the networks by initiating a compromise between the number of extra input/output ports required and the number of extra switching points, and improves the design flexibility. With the

$$\delta\text{SPP}^{\text{Case1}} = \frac{\sum_{b\in N}\left[K\cdot(\Omega_b)^2 - K\cdot\left(\Omega_b^0\right)^2\right]}{\sum_{b\in N} K\cdot\left(\Omega_b^0\right)^2} = \frac{\sum_{b\in N}\left[(\Omega_b)^2 - \left(\Omega_b^0\right)^2\right]}{\sum_{b\in N}\left(\Omega_b^0\right)^2} \tag{30}$$

$$\begin{aligned}\delta\text{SPP}^{\text{Case2}} &= \frac{\sum_{b}\left[2\cdot\left(\Omega_b^0 + F_b^F + F_b^B\right)^2 + 2\cdot B\cdot\left(\Omega_b^0 + F_b^B\right)^2 + K\cdot\left(\Omega_b^0\right)^2\right] - \sum_b K\cdot\left(\Omega_b^0\right)^2}{\sum_b K\cdot\left(\Omega_b^0\right)^2} \\ &= \frac{2\cdot\sum_b\left[\left(\Omega_b^0 + F_b^F + F_b^B\right)^2 + B\cdot\left(\Omega_b^0 + F_b^B\right)^2\right]}{K\cdot\sum_b\left(\Omega_b^0\right)^2}\end{aligned} \tag{31}$$

$$\delta\text{SPP}^{\text{Case3}} = \frac{\sum_b\left[2\cdot\left(\Omega_b^0 + F_b^F\right)^2 + K\cdot\left(\Omega_b^0\right)^2\right] - \sum_b K\cdot\left(\Omega_b^0\right)^2}{\sum_b K\cdot\left(\Omega_b^0\right)^2} = \frac{2\cdot\sum_b\left[\left(\Omega_b^0 + F_b^F\right)^2\right]}{K\cdot\sum_b\left(\Omega_b^0\right)^2} \tag{32}$$

same number of switching points as traffic is growing, the case with waveband- and fiber-switching tiers requires much less input/output ports than the case with only fiber-switching tier especially when the networks are sparsely meshed.

VI. Conclusion

This paper has demonstrated a novel approach to dimensioning network capacity, where a switch architecture of MG-OXCs is adopted. To improve the scalability in manufacturing and maintenance for the switch core, the proposed design method expands the switching capacity in the waveband- and fiber-switching tiers instead of only the lambda-switching tier. We formulated the problem of RWAT into a CP according to traffic matrices. To avoid the very high computation complexity in solving the CP, we proposed a heuristic approach where the optimization process is approximated by three subtasks that can be sequentially performed. Thus, the whole optimization process is simplified to just performing two ILP processes. We first conducted an experiment to compare the proposed heuristic approach with the CP process in Section III, and found that the heuristic approach can achieve a very good approximation of the optimal solution. Then experiments on four networks were conducted to further verify the proposed design approach. The experiment results showed that the MG-OXC networks may require more input/output ports than using pure lambda-switching OXCs. However, the increase in the number of switching points (or the number of mirrors with 2-D flexibility in the MEMS technology adopted in this study) as the traffic is growing can be largely slowed, so as to improve the network scalability. We also observed from the experimental results that with the same number of switching points, the case with waveband- and fiber-switching tiers required much less input/output ports than the case with only fiber-switching tier especially when the networks are sparsely meshed. The proposed heuristic approach can effectively solve the RWAT problem. Expanding networks with tunnel tiers compromise between the size of switching fabrics and the number of input/output ports in OXCs, where the scalability in manufacturing and maintenance for the switch fabrics can be improved. Our future study will consider sublambda traffic in the MG-OXC networks and the networks of multiple waveband-switching tiers with different traffic granularity.

References

[1] P.-H. Ho and H. T. Mouftah, "Routing and wavelength assignment with multi-granularity traffic in optical networks," *IEEE J. Lightwave Technol.*, vol. 20, pp. 1292–1303, Aug. 2002.

[2] E. Mannie *et al.*. (2002) Generalized multi-protocol label switching (GMPLS) architecture. [Online]. Available: draft-ietf-ccamp-gmpls-architecture-02.txt

[3] M. Lee, J. Yu, Y. Kim, C.-H. Kang, and J. Park, "Design of hierarchical crossconnect WDM networks employing a two-stage multiplexing scheme of waveband and wavelength," *IEEE J. Select. Areas Commun.*, vol. 20, pp. 166–171, Jan. 2002.

[4] O. Gerstel, R. Ramaswami, and W.-K. Wang, "Making use of a two-stage multiplexing scheme in a WDM network," presented at the Optical Fiber Communications (OFC'00), Baltimore, MD, Mar. 2000, ThD1.1-ThD1.3.

[5] L. Noirie, M. Vigoureus, and E. Dotaro, "Impact of intermediate traffic grouping on the dimensioning of multi-granularity optical networks," presented at the Optical Fiber Communications (OFC'01), Anaheim, CA, Mar. 2001, TuG3.1-TuG3.3.

[6] P.-H. Ho and H. T. Mouftah, "Path selection with tunnel allocation in the optical Internet based on generalized MPLS architecture," in *Proc. IEEE Int. Communications Conf. (ICC'02)*, Apr. 2002, pp. 2697–2701.

[7] X. Cao, Y. Xiong, V. Anand, and C. Qiao, "Wavelength band switching in multi-granularity all-optical networks," in *Proc. SPIE OPTICOMM'02*, Boston, MA, July 2002, pp. 198–210.

[8] G. Shen, T. H. Cheng, S. K. Bose, C. Lu, and T. Y. Chai, "Architectural design for multistage 2-D MEMS optical switches," *IEEE J. Lightwave Technol.*, vol. 20, pp. 178–187, Feb. 2002.

[9] *ILOG CPLEX 7.1 – Advanced Reference Manual*, ILOG, 2001.

[10] H. T. Mouftah and P.-H. Ho, *Optical Networks – Architectures and Survivability*. Norwell, MA: Kluwer, 2002.

Pin-Han Ho (S'01–M'02) received the B.Sc. and M.Sc. degrees in electrical and computer engineering from the National Taiwan University, Taipei, in 1993 and 1995, respectively, and the Ph.D. degree from Queen's University, Kingston, Canada, in 2002, focusing on the optical communications systems, survivable networking, and quality-of-service (QoS) routing problems.

In 2002, he joined the Electrical and Computer Engineering Department, University of Waterloo, Waterloo, ON, Canada, as an Assistant Professor. He is the first author of more than 40 refereed technical papers and the coauthor of a book on optical networking and survivability.

Dr. Ho is the recipient of the Best Paper Award and the Outstanding Paper Award from SPECTS 2002 and HPSR 2002, respectively.

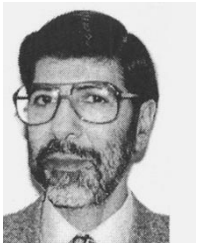

Hussein Mouftah (S'74–M'76–SM'80–F'90) joined the School of Information Technology and Engineering (SITE), University of Ottawa, Ottawa, ON, Canada, in September 2002, as a Canada Research Chair Professor (Tier 1). From 1979, he was with the Department of Electrical and Computer Engineering, Queen's University, Kingston, ON, Canada, where he was prior to his departure in August 2002, a Full Professor and the Department Associate Head, after three years of industrial experience mainly at Bell Northern Research, Ottawa, ON, Canada (now Nortel Networks). He has spent three sabbatical years also at Nortel Networks (1986–1987, 1993–1994, and 2000–2001), conducting research in the area of broadband packet switching networks, mobile wireless networks, and quality-of-service over the optical Internet. He is the author or coauthor of three books and more than 650 technical papers and eight patents in this area.

Dr. Mouftah served as Editor-in-Chief of the IEEE *Communications Magazine* (1995–1997) and the IEEE Communications Society Director of Magazines (1998–1999). He is the recipient of the 1989 Engineering Medal for Research and Development of the Association of Professional Engineers of Ontario (PEO). He is the joint holder of the Best Paper Award for a paper presented at SPECTS 2002, and the Outstanding Paper Award for papers presented at the IEEE HPSR 2002 and the IEEE ISMVL 1985. He is the joint holder of a Honorable Mention for the Frederick W. Ellersick Price Paper Award for Best Paper in the IEEE Communications Magazine in 1993. He is the recipient of the IEEE Canada (Region 7) Outstanding Service Award (1995).

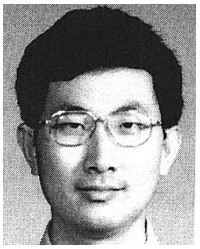

Jing Wu (M'98) received the Ph.D. degree in systems engineering from Xian Jiao Tong University, Xian, China, in 1997.

He has been a Research Scientist in the Communications Research Center Canada, Ottawa, ON, Canada, since 2001. His research interests mainly include control and management of optical networks, protocols and algorithms in networking, network performance evaluation and optimization, etc. In the past, he worked at Beijing University of Posts and Telecommunications, Beijing, China, as an Assistant Professor, Queen's University, Kingston, ON, Canada, as a Postdoctoral Fellow, and Nortel Networks Corporate, Ottawa, ON, Canada, as a System Design Engineer.

Dr. Wu is a Member of the Society of Computer Simulation.